Plasma diagnostics and simulations

Determination of titanium atom and ion densities in sputter deposition plasmas by optical emission spectroscopy

Tasks

1. Measure the overview optical emission spectrum (300 – 800 nm) in dcMS and HiPIMS discharge for two sets of experimental conditions – 1 Pa, 0.5 kW and 5 Pa, 1.5 kW; identify the spectral lines in the ranges of 320 – 340 nm, 360 – 380 nm, 430 – 480 nm and 690 – 800 nm.
2. Determine the titanium atom and ion number densities of HiPIMS discharge at 5 Pa and 1.5 kW from two chosen sets of spectral lines measured in task 1.
3. Measure the intensities of selected titanium atom spectral lines in dcMS as a function of applied power for the pressure of 5 Pa and as a function of working pressure for the applied power of 1.5 kW. Determine the evolution of titanium atom number densities using EBF method and compare it to the evolution of titanium atom spectral line (399.86 nm) intensity.
4. Measure the evolutions of titanium atom and ion spectral lines as a function of duty cycle (from dcMS to HiPIMS discharge) and determine the titanium atom and titanium ion number densities.
5. Study the reproducibility of the experiment. Measure a selected spectra 10 times with only 1 accumulation and ones with 10 accumulations. Compare the evolution of spectral lines intensities and calculated number densities for averaged and non-averaged spectra.

Introduction

Plasma is optically active medium, where the light can be either generated or absorbed. Usually, the ideal plasma is assumed, where the light is only generated or only absorbed while the second effect is neglected. However, in the real plasma both events can occur simultaneously. The process in which some of the radiation emitted by plasma is absorbed by the plasma itself is called self-absorption. The effect of self-absorption causes the decrease of the plasma emissivity. Only spectral transition ending at the energy state with the long time of life such as ground or metastable states can suffer from the self-absorption. The simulation of intensities of two titanium atom resonant lines computed not taking and taking into account the effect of self-absorption is depicted in figure 1a) and 1b), respectively. The self-absorption depends on the line strength, length of the absorbing media and on the number of particles capable to absorb the emitted photon.

Effective branching fractions method

Theory

The method of effective branching fractions (EBF method) was developed originally for measurement of metastable and resonant state densities of argon atoms from self-absorbed optical

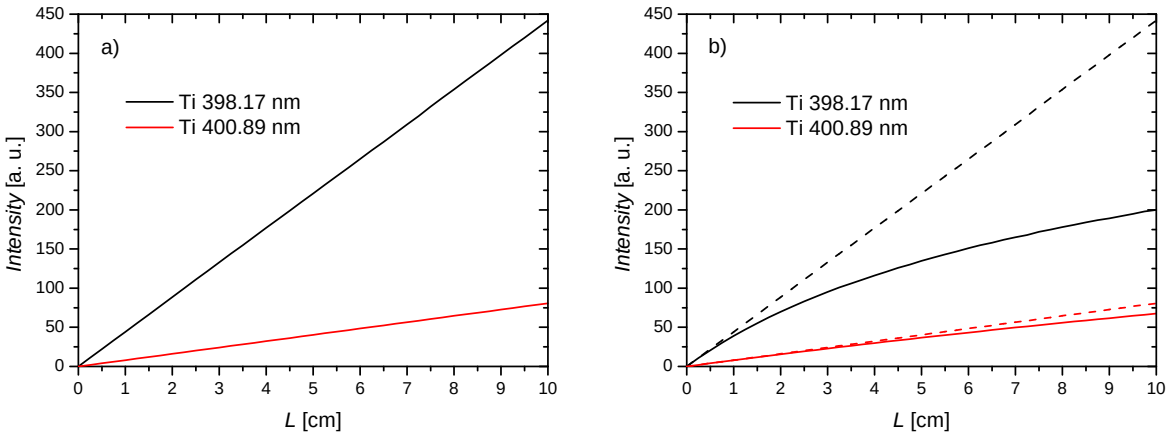

Figure 1: Simulated evolution of two titanium atom resonant spectral lines intensities with the length of optically active media a) without self-absorption and b) with self-absorption of the radiation.

emission spectra [1, 2]. In contrast to absorption methods measuring the attenuation of light passing through the plasma from an external light source, self-absorption methods consider the studied plasma as both light emitting and absorbing medium. When optical depth of a transition is $kL \gtrsim 1$ (k is absorption coefficient and L is plasma depth in the direction of observation), photons emitted in the discharge may be significantly re-absorbed by atoms in the lower state of the transition before escaping the plasma. Unlike classical self-absorption methods comparing intensities of transitions with the same lower level, the EBF method compares intensities of transitions from a common upper level i by means of branching fractions

$$\Gamma_{ij} = \frac{\Phi_{ij}}{\sum_l \Phi_{il}}, \tag{1}$$

where Φ_{ij} is photon emission rate of transition $i \to j$ and the summing is performed over all possible lower states l. In the absence of absorption, the photon emission rates are simply proportional to the product of Einstein coefficient for spontaneous emission A_{ij} and the number of atoms in the excited states. The branching fractions equal

$$\Gamma_{ij}^{\text{free}} = \frac{A_{ij}}{\sum_l A_{il}}, \tag{2}$$

the branching fractions for absorption-free plasma are therefore simply determined by the Einstein coefficients of spontaneous emission.

When the self-absorption of radiation occurs in plasma, apparent branching fractions of escaping radiation may be altered, since the light of different transitions is absorbed to a different extent. The self-absorption in plasma is often estimated using the concept of escape factors developed by Holstein [3]. The effective branching fraction of spectral line in the presence of self-absorption is calculated as

$$\Gamma_{ij}^{\text{eff}} = \frac{g(k_{ij}^0 L) A_{ij}}{\sum_l g(k_{il}^0 L) A_{il}}, \tag{3}$$

where g is the (radiation) escape factor depending on the absorption coefficient k_{il}^0 evaluated at the spectral line centre and L is a sensed plasma depth. The EBF method was applied on magnetron sputtering system [4], where the accurate evaluation of self-absorption is a non-trivial problem. In order to keep the method simple, the commonly used approximative formula of Mewe [5] was adopted

$$g(k_{ij}^0 L) = \frac{2 - \mathrm{e}^{-k_{ij}^0 L/1000}}{1 + k_{ij}^0 L}. \tag{4}$$

The formula assumes a uniform spatial distribution of atoms in both upper and lower states of transition. In our case, the distributions of atoms in chamber are inhomogeneous with most of the atoms located just above the racetrack. When the optical fibre is directed along the tangent line of the race track (and parallel with the target), the fibre senses a region of enhanced density of a depth L. This value is taken into calculations as the absorption path; however, the uncertainty of this absorption path determination can contribute significantly to the measurement error. Since Doppler broadening is the dominant broadening mechanism at pressure of $\approx 1\,\mathrm{Pa}$, the absorption coefficient k_{il}^0 at the line centre is calculated as

$$k_{ij}^0 = \frac{\lambda_{ij}^3}{8\pi^{3/2}} \sqrt{\frac{m_0}{2k_\mathrm{b}T}} \frac{g_i}{g_j} A_{ij} n_j, \tag{5}$$

in which m_0 is atomic mass, λ_{ij} wavelength of the transition in the line center, T is kinetic temperature of atoms and g_i and g_j are statistical weights of upper and lower level, respectively. The density of the lower state n_j is the searched unknown quantity.

In order to determine the density of a specific atomic state, intensities of spectral lines of spontaneous transitions ending in the studied state and of their competitive transitions from the same upper level must be measured. Since such transitions will end on several lower states, several densities n_j are typically simultaneously determined. It is recommended to measure more spectral lines and fit the effective branching fractions (3) by least squares method to the measured values

$$\Gamma_{ij}^{\mathrm{exp}} = \frac{I_{ij}/h\nu_{ij}}{\sum_l I_{il}/h\nu_{il}}. \tag{6}$$

$h\nu_{ij}$ are photon energies. The measured intensities I_{ij} should be corrected for spectrometer spectral sensitivity and integrated over the spectral profiles.

For ease of use the *EBF fit* software, enabling the calculation of branching fractions from measured line intensities and their fit by the least squares method, was developed [6]. The software enables us to determine the titanium atom and ion ground state density from optical emission spectra. A database of spectral lines with wavelengths, Einstein coefficients, statistical weights etc. needed for calculation of branching fractions of titanium atom and ion is included in the software.

Application to ground state Ti atoms

The ground state of titanium neutral atom, originating from electron configuration $1s^2 2s^2 2p^6 3s^2 3p^6 3d^2 4s^2$, is a $^3\mathrm{F}_2$. Other levels a $^3\mathrm{F}_3$ and a $^3\mathrm{F}_4$ of the triplet term lie 0.021 and 0.048 eV above the ground state, respectively.

The optical spectrum of titanium in UV-VIS range is plentiful. The selected spectral lines sorted according to their upper state, fulfilling the condition of one transition going to the ground state, are summarized in 1. The utilizable lines have to meet several requirements: high transition probability (Einstein coefficient of spontaneous emission), no overlapping with surrounding spectral features in the measured spectra, ease of measurement and instrument calibration etc. Close wavelengths provide a low impact of varying instrument sensitivity on the measured intensity values.

The selected transitions of neutral Ti atom with their upper and lower levels are shown in a diagram in 3a). In order to calculate the effective branching fractions from formula (3), the densities of all three a $^3\mathrm{F}$ levels must be taken into account. Since the energy splitting of the levels is low, the levels are assumed to be in local thermodynamic equilibrium with the densities following the Boltzmann law

$$n_j = n_0 \frac{g_j}{g_0} \mathrm{e}^{-\frac{E_j - E_0}{k_\mathrm{b} T_\mathrm{exc}}},$$

where T_exc is excitation temperature of a ^{3}F triplet state and n_0 is density of a $^3\mathrm{F}_2$ level. By fitting 13 branching fractions of selected transitions (see table 1), n_0 and T_exc quantities are determined. Since populations of a $^3\mathrm{F}_3$ and a $^3\mathrm{F}_4$ levels are not negligible, the sum of densities of all three levels is taken as the resulting density of titanium atoms [Ti].

Application to ground state Ti ions

The ground state of singly ionized titanium, originating from electron configuration $1s^2 2s^2 2p^6 3s^2 3p^6 3d^2 4s$, is a $^4\mathrm{F}_{3/2}$. Other levels a $^4\mathrm{F}_{5/2}$, a $^4\mathrm{F}_{7/2}$ and a $^4\mathrm{F}_{9/2}$ of the quartet term lie 0.012, 0.028 and 0.049 eV above the ground state, respectively.

Spectral lines of Ti ion sorted according to their upper state, fulfilling the condition of one transition going to the ground state, are summarized in table 2, 19 selected transitions with their upper and lower levels are shown in a diagram in 3b). In order to calculate the effective branching fractions, densities of all a ^{4}F levels must be evaluated. As in case of neutral titanium, Boltzmann law is taken to decrease the number of fitted parameters. The sum of densities of all four levels is taken as the resulting density of titanium ions [Ti^+].

Magnetron sputtering

Magnetron sputtering belongs to the group of physical vapor deposition (PVD) techniques, which generally involve the condensation of vapor created from a solid state source, often in the presence of a glow discharge or plasma. Nowadays, in many cases the magnetron sputtered films outperform the films deposited by other PVD processes offering the same functionality as much thicker films produced by other coating techniques. Thin films deposited by magnetron sputtering find application in numerous technological domains including hard, wear-resistant, optical, corrosion-resistant coatings or coatings for microelectronics, etc.

The sputtering process is shown in figure 2. The ions are generated in plasma and are accelerated by the electric field towards the target surface. The incident ion bombards the target surface causing collision cascade resulting in physical ejection of atoms or small clusters of atoms from the target surface which are deposited onto substrate.

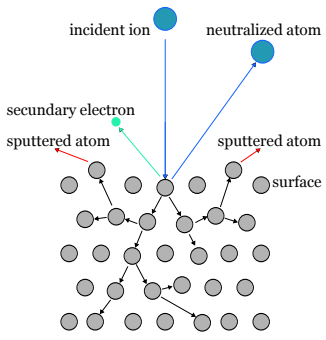

Figure 2: Diagram of sputtering process.

Before being deposited onto the samples, the film forming species should follow a certain pathway. On their pathway these particles may be ionized, neutralized or they can chemically react with other particles in the gas phase. During their transport, it is also very likely that they exhibit gas-phase collisions with background gas atoms.

High power impulse magnetron sputtering (HiPIMS) is one of the PVD techniques. The applied power is focused into a short pulse (microseconds or 10's of microseconds) or into a long

pulse (hundreds of microseconds), but both with duty cycles less than 5%. In HiPIMS, very high instantaneous power density (several $\mathrm{kW\,cm^{-2}}$) is applied to the target, while keeping an averaged power density similar to the one used in conventional dc magnetron sputtering (dcMS). Higher actual applied power results in higher plasma density and hence higher fraction of ionized sputtered species compared to dcMS, which is the major advantage of HiPIMS. Coatings prepared by HiPIMS have improved properties in terms of film density, adhesion, surface roughness and higher hardness.

Experimental setup

The measurements is done on the magnetron sputtering system Alcatel SCM 650. The sputtering system is equipped with Ti target (99.95% purity) of rectangular shape ($25\times7.5\,\mathrm{cm}$) and unbalanced magnetic field configuration. The discharge is powered by a Melec SIPP 2000 HiPIMS generator operated in both dcMS and HiPIMS mode. The Melec generator is equipped with a current and voltage probe for electric measurements.

The deposition chamber is evacuated by a turbo-molecular pump backed with a Roots pump down to a pressure of 10^{-4} Pa. The buffer gas is argon (99.999%). The working pressure can be varied from 0.3 Pa to 5.4 Pa by the gas flow-meter ($1-140\,\mathrm{sccm}$) and measured by MKS Baratron.

The optical emission spectroscopy (OES) is carried out using a Andor Shamrock spectrometer (Czerny-Turner configuration) with 0.75 m focal length, $2400\,\mathrm{grooves.mm^{-1}}$ grating and CCD detector. The total integration time is set to achieve sufficient line intensities. The optical fiber is placed on a movable holder to collect the light from 10 mm above the target and it is directed along the tangent line of the racetrack paralell with the target to achieve the longest optical depth.

Measurement and data processing

Measurement

- Turn on spectrometer.
- Turn on cooling of magnetron and generator.
- Set working pressure.
- Turn on generator (program Melec).
- Set arc limit.
- Set operation mode (dcMS, HiPIMS), and pulse parameters.
- Set discharge parameters (voltage, current, power).
- Ignite discharge.

Data processing

- Identify the selected spectral lines and determine their intensities (for example using Spectrum analyzer [8, 9]).
- Create *.txt file with two columns - wavelength and corresponding intensity
- Determine [Ti] or [Ti^+] using EBF fit, $L \approx 23\,\mathrm{cm}$, $T \approx 500\,\mathrm{K}$, fit also T_{exc}.
- For spectral line intensity evolution, normalize spectra for the same integration time and number of accumulations.

References

[1] Schulze M, Yanguas-Gil A, von Keudell A and Awakowicz P 2008 *J. Phys. D: Appl. Phys.* **41** 065206

[2] Boffard J B, Jung R O, Lin C C and Wendt A E 2009 *Plasma Sources Sci. Technol.* **18** 035017

[3] Holstein T 1947 *Phys. Rev.* **72** 1212

[4] Vašina P, Fekete M, Hnilica J, Klein P, Dosoudilová L, Dvořák P and Navrátil Z 2015 *Plasma Sources Sci. Technol.* **24** 065022

[5] Mewe R 1967 *Br. J. Appl. Phys.* **18** 107

[6] Software EBF fit. `http://www.physics.muni.cz/~zdenek/ebffit/`

[7] Kramida A, Ralchenko Yu, Reader J and NIST ASD Team 2018. *NIST Atomic Spectra Database (ver. 5.5.6)* [Online] `http://physics.nist.gov/asd`.

[8] Navrátil Z, Trunec D, Šmíd R and Lazar L 2006 *Czech. J. Phys.* **56** B944–51

[9] Software Spectrum Analyzer `http://www.physics.muni.cz/~zdenek/span/`

Appendix

Transition	λ (nm)	A_{ij} (10^7 s^{-1})	Γ_{ij}
$3d^2(^3\mathrm{P})4\mathrm{s}4\mathrm{p}(^3\mathrm{P}^\circ)$ z $^5\mathrm{S}^\circ_2 \rightarrow 3d^2 4s^2$ a $^3\mathrm{F}_2$	398.24806	0.45000	0.764
$3d^2(^3\mathrm{P})4\mathrm{s}4\mathrm{p}(^3\mathrm{P}^\circ)$ z $^5\mathrm{S}^\circ_2 \rightarrow 3d^2 4s^2$ a $^3\mathrm{F}_3$	400.96565	0.13900	0.236
$3d^2(^3\mathrm{F})4\mathrm{s}4\mathrm{p}(^1\mathrm{P}^\circ)$ y $^3\mathrm{F}^\circ_2 \rightarrow 3d^2 4s^2$ a $^3\mathrm{F}_2$	398.17616	4.42000	0.846
$3d^2(^3\mathrm{F})4\mathrm{s}4\mathrm{p}(^1\mathrm{P}^\circ)$ y $^3\mathrm{F}^\circ_2 \rightarrow 3d^2 4s^2$ a $^3\mathrm{F}_3$	400.89273	0.80700	0.154
$3d^2(^3\mathrm{F})4\mathrm{s}4\mathrm{p}(^1\mathrm{P}^\circ)$ y $^3\mathrm{F}^\circ_3 \rightarrow 3d^2 4s^2$ a $^3\mathrm{F}_2$	396.28508	0.47100	0.083
$3d^2(^3\mathrm{F})4\mathrm{s}4\mathrm{p}(^1\mathrm{P}^\circ)$ y $^3\mathrm{F}^\circ_3 \rightarrow 3d^2 4s^2$ a $^3\mathrm{F}_3$	398.97586	4.48000	0.794
$3d^2(^3\mathrm{F})4\mathrm{s}4\mathrm{p}(^1\mathrm{P}^\circ)$ y $^3\mathrm{F}^\circ_3 \rightarrow 3d^2 4s^2$ a $^3\mathrm{F}_4$	402.45709	0.69100	0.122
$3d^2(^3\mathrm{F})4\mathrm{s}4\mathrm{p}(^1\mathrm{P}^\circ)$ y $^3\mathrm{F}^\circ_4 \rightarrow 3d^2 4s^2$ a $^3\mathrm{F}_3$	396.42694	0.36400	0.070
$3d^2(^3\mathrm{F})4\mathrm{s}4\mathrm{p}(^1\mathrm{P}^\circ)$ y $^3\mathrm{F}^\circ_4 \rightarrow 3d^2 4s^2$ a $^3\mathrm{F}_4$	399.86366	4.81000	0.930
$3d^3(^4\mathrm{F})4\mathrm{p}$ y $^3\mathrm{D}^\circ_2 \rightarrow 3d^2 4s^2$ a $^3\mathrm{F}_2$	392.98740	0.85100	0.197
$3d^3(^4\mathrm{F})4\mathrm{p}$ y $^3\mathrm{D}^\circ_2 \rightarrow 3d^2 4s^2$ a $^3\mathrm{F}_3$	395.63343	3.46000	0.803
$3d^3(^4\mathrm{F})4\mathrm{p}$ y $^3\mathrm{D}^\circ_3 \rightarrow 3d^2 4s^2$ a $^3\mathrm{F}_3$	392.45268	0.81000	0.141
$3d^3(^4\mathrm{F})4\mathrm{p}$ y $^3\mathrm{D}^\circ_3 \rightarrow 3d^2 4s^2$ a $^3\mathrm{F}_4$	395.82016	4.88000	0.852

Table 1: Einstein coefficients of spontaneous emission and branching fractions for transitions of isolated titanium atom [7]. Lines are divided into groups with a common upper level.

Transition	λ (nm)	A_{ij} (10^7 s^{-1})	Γ_{ij}
$3d^2(^3\mathrm{F})4\mathrm{pz}\ ^4\mathrm{G}^\circ_{5/2} \rightarrow 3d^2(^3\mathrm{F})4s\ \mathrm{a}\ ^4\mathrm{F}_{3/2}$	338.37584	13.90000	0.833
$3d^2(^3\mathrm{F})4\mathrm{p}\ \mathrm{z}\ ^4\mathrm{G}^\circ_{5/2} \rightarrow 3d^2(^3\mathrm{F})4s\ \mathrm{a}\ ^4\mathrm{F}_{5/2}$	339.45721	2.69000	0.161
$3d^2(^3\mathrm{F})4\mathrm{p}\ \mathrm{z}\ ^4\mathrm{G}^\circ_{7/2} \rightarrow 3d^2(^3\mathrm{F})4s\ \mathrm{a}\ ^4\mathrm{F}_{5/2}$	337.27927	14.10000	0.830
$3d^2(^3\mathrm{F})4\mathrm{p}\ \mathrm{z}\ ^4\mathrm{G}^\circ_{7/2} \rightarrow 3d^2(^3\mathrm{F})4s\ \mathrm{a}\ ^4\mathrm{F}_{7/2}$	338.78334	2.81000	0.165
$3d^2(^3\mathrm{F})4\mathrm{p}\ \mathrm{z}\ ^4\mathrm{G}^\circ_{9/2} \rightarrow 3d^2(^3\mathrm{F})4s\ \mathrm{a}\ ^4\mathrm{F}_{7/2}$	336.12121	15.80000	0.920
$3d^2(^3\mathrm{F})4\mathrm{p}\ \mathrm{z}\ ^4\mathrm{G}^\circ_{9/2} \rightarrow 3d^2(^3\mathrm{F})4s\ \mathrm{a}\ ^4\mathrm{F}_{9/2}$	338.02766	1.37000	0.080
$3d^2(^3\mathrm{F})4\mathrm{p}\ \mathrm{z}\ ^4\mathrm{F}^\circ_{3/2} \rightarrow 3d^2(^3\mathrm{F})4s\ \mathrm{a}\ ^4\mathrm{F}_{3/2}$	324.19825	14.70000	0.782
$3d^2(^3\mathrm{F})4\mathrm{p}\ \mathrm{z}\ ^4\mathrm{F}^\circ_{3/2} \rightarrow 3d^2(^3\mathrm{F})4s\ \mathrm{a}\ ^4\mathrm{F}_{5/2}$	325.19078	4.09000	0.218
$3d^2(^3\mathrm{F})4\mathrm{p}\ \mathrm{z}\ ^4\mathrm{F}^\circ_{7/2} \rightarrow 3d^2(^3\mathrm{F})4s\ \mathrm{a}\ ^4\mathrm{F}_{5/2}$	322.28413	3.07000	0.162
$3d^2(^3\mathrm{F})4\mathrm{p}\ \mathrm{z}\ ^4\mathrm{F}^\circ_{7/2} \rightarrow 3d^2(^3\mathrm{F})4s\ \mathrm{a}\ ^4\mathrm{F}_{9/2}$	325.42453	2.17000	0.115
$3d^2(^3\mathrm{F})4\mathrm{p}\ \mathrm{z}\ ^4\mathrm{F}^\circ_{9/2} \rightarrow 3d^2(^3\mathrm{F})4s\ \mathrm{a}\ ^4\mathrm{F}_{7/2}$	321.70543	2.09000	0.109
$3d^2(^3\mathrm{F})4\mathrm{p}\ \mathrm{z}\ ^4\mathrm{F}^\circ_{9/2} \rightarrow 3d^2(^3\mathrm{F})4s\ \mathrm{a}\ ^4\mathrm{F}_{9/2}$	323.45146	17.10000	0.891
$3d^2(^3\mathrm{F})4\mathrm{p}\ \mathrm{z}\ ^2\mathrm{D}^\circ_{5/2} \rightarrow 3d^2(^3\mathrm{F})4s\ \mathrm{a}\ ^4\mathrm{F}_{5/2}$	313.07985	0.82000	0.547
$3d^2(^3\mathrm{F})4\mathrm{p}\ \mathrm{z}\ ^2\mathrm{D}^\circ_{5/2} \rightarrow 3d^2(^3\mathrm{F})4s\ \mathrm{a}\ ^4\mathrm{F}_{7/2}$	314.37546	0.62000	0.414
$3d^2(^3\mathrm{F})4\mathrm{p}\ \mathrm{z}\ ^4\mathrm{D}^\circ_{5/2} \rightarrow 3d^2(^3\mathrm{F})4s\ \mathrm{a}\ ^4\mathrm{F}_{3/2}$	305.73929	0.19800	0.012
$3d^2(^3\mathrm{F})4\mathrm{p}\ \mathrm{z}\ ^4\mathrm{D}^\circ_{5/2} \rightarrow 3d^2(^3\mathrm{F})4s\ \mathrm{a}\ ^4\mathrm{F}_{7/2}$	307.86442	13.40000	0.807
$3d^2(^3\mathrm{F})4\mathrm{p}\ \mathrm{z}\ ^4\mathrm{D}^\circ_{7/2} \rightarrow 3d^2(^3\mathrm{F})4s\ \mathrm{a}\ ^4\mathrm{F}_{5/2}$	305.97353	0.24000	0.014
$3d^2(^3\mathrm{F})4\mathrm{p}\ \mathrm{z}\ ^4\mathrm{D}^\circ_{7/2} \rightarrow 3d^2(^3\mathrm{F})4s\ \mathrm{a}\ ^4\mathrm{F}_{7/2}$	307.21071	2.13000	0.123
$3d^2(^3\mathrm{F})4\mathrm{p}\ \mathrm{z}\ ^4\mathrm{D}^\circ_{7/2} \rightarrow 3d^2(^3\mathrm{F})4s\ \mathrm{a}\ ^4\mathrm{F}_{9/2}$	308.80256	15.00000	0.864

Table 2: Einstein coefficients of spontaneous emission and branching fractions for transitions of titanium ion [7]. Lines are divided into groups with a common upper level.

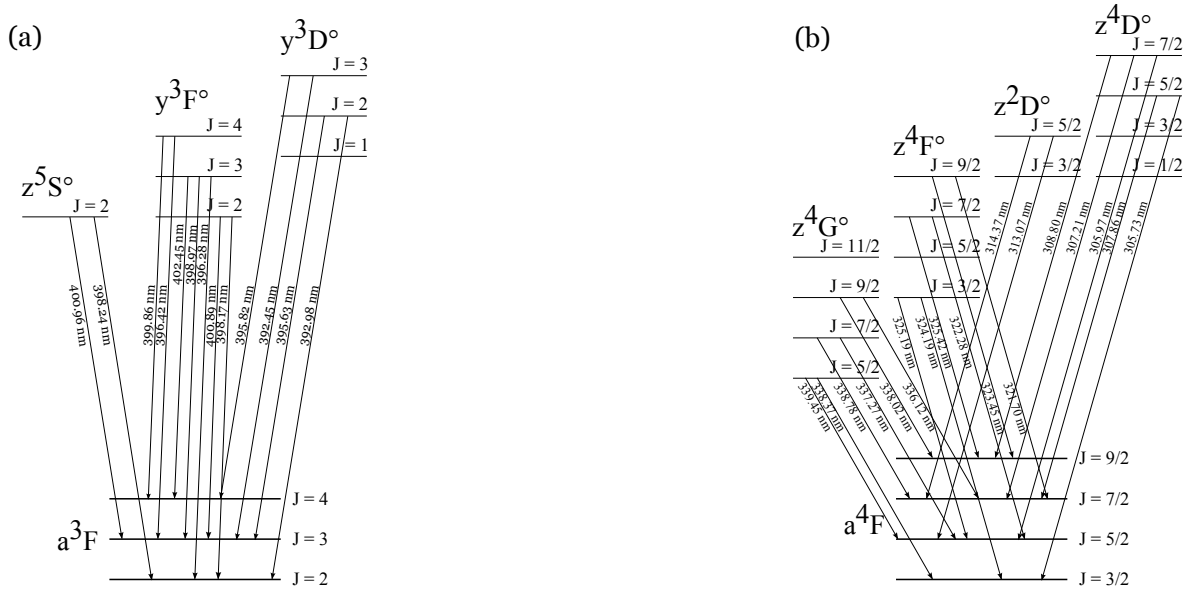

Figure 3: Energy levels and selected transitions for density measurement of a) Ti neutral atom and b) Ti ion.